



A Link between Ram Pressure Stripping and Active Galactic Nuclei

Angelo Ricarte^{1,2} , Michael Tremmel³ , Priyamvada Natarajan^{4,5} , and Thomas Quinn⁶

¹ Center for Astrophysics|Harvard & Smithsonian, 60 Garden Street, Cambridge, MA 02138, USA; angelo.ricarte@cfa.harvard.edu

² Black Hole Initiative, 20 Garden Street, Cambridge, MA 02138, USA

³ Yale Center for Astronomy and Astrophysics, Physics Department, Yale University, P.O. Box 208120, New Haven, CT 06520, USA

⁴ Department of Astronomy, Yale University, 52 Hillhouse Avenue, New Haven, CT 06511, USA

⁵ Department of Physics, Yale University, P.O. Box 208121, New Haven, CT 06520, USA

⁶ Department of Astronomy, University of Washington, P.O. Box 351580, Seattle, WA 98195, USA

Received 2020 March 11; revised 2020 May 5; accepted 2020 May 5; published 2020 May 19

Abstract

The dense environment of a galaxy cluster can radically transform the content of in-falling galaxies. Recent observations have found a significant population of active galactic nuclei (AGN) within “jellyfish galaxies,” galaxies with trailing tails of gas and stars that indicate significant ram pressure stripping. The relationship between AGN and ram pressure stripping is not well understood. In this Letter, we investigate the connection between AGN activity and ram pressure in a fully cosmological setting for the first time using the ROMULUSC simulation, one of the highest resolution simulations of a galaxy cluster to date. For lower mass galaxies (with stellar masses $M_* \lesssim 10^{9.5} M_\odot$) both star formation and black hole accretion are suppressed by ram pressure before they reach pericenter, whereas for more massive galaxies accretion onto the black hole is enhanced during pericentric passage. Our analysis also indicates that as long as the galaxy retains gas, AGN with higher Eddington ratios are more likely to be found in galaxies experiencing higher ram pressure. We conclude that prior to quenching star formation, ram pressure triggers enhanced accretion onto the black hole, which in our model then produces heating and outflows due to AGN feedback. These simulations suggest that AGN feedback may in turn serve to aid in the quenching of star formation in tandem with ram pressure.

Unified Astronomy Thesaurus concepts: Active galactic nuclei (16); AGN host galaxies (2017); Supermassive black holes (1663); Galaxy clusters (584); Galaxy quenching (2040)

1. Introduction

As clusters of galaxies assemble, they dynamically transform the physical properties of in-falling cluster members. Galaxies falling into a cluster experience ram pressure from dense intracluster medium (ICM) gas that can potentially unbind their individual gas reservoirs (Gunn et al. 1972). This process referred to as ram pressure stripping (RPS) can eventually remove a galaxy’s entire gas supply, making it an important quenching pathway for satellite galaxies (Vollmer et al. 2001; Tonnesen et al. 2007). Observationally, RPS results in disturbed galaxy morphologies and trailing tails of stripped gas (e.g., Kenney et al. 2004; van Gorkom 2004; Cramer et al. 2019). The most extreme examples have been dubbed “jellyfish” galaxies, due to the evocative morphologies of their star-forming tails (Ebeling et al. 2014; Boselli et al. 2016; Poggianti et al. 2016). Prior to complete gas removal, moderate values of ram pressure have also been shown to increase the star formation rate in galaxies both observed (Crowl & Kenney 2006; Merluzzi et al. 2013; Vulcani et al. 2018) and simulated (Kronberger et al. 2008; Kapferer et al. 2009; Tonnesen & Bryan 2009; Bekki 2014). In this picture, the increased pressure initially helps compress the gas and triggers increased star formation. Other proposed processes for accretion of gas to the centers of galaxies include gravitational instabilities and the inspiral of preferentially low angular momentum clumps that lose angular momentum to a wind: drag from the nonrotating ICM operating on dense clumps (Schulz & Struck 2001; Tonnesen & Bryan 2009; Ramos-Martínez et al. 2018). Over time, the interstellar medium (ISM) is fully stripped from the galaxy and star formation ceases. Recently, a very high incidence of AGN (5/7) has been

observed in a sample of jellyfish galaxies (Poggianti et al. 2017), and comprehensive follow-up of this sample has led to the identification of AGN-driven outflows (Radovich et al. 2019) and a compelling case for AGN feedback in action (George et al. 2019). It is plausible that the same mechanisms that initially promote star formation can also fuel active galactic nuclei (AGN) during the ram pressure stripping process. Indeed, outside of cluster environments, ram pressure induced shocks are known to produce nuclear inflows that can fuel AGN in the context of galaxy merger simulations (Barnes 2002; Capelo & Dotti 2017; Blumenthal & Barnes 2018).

In this work, we investigate the connection between ram pressure stripping and AGN using a high-resolution hydrodynamical cluster simulation for the first time. ROMULUSC is one of the highest resolution cosmological simulations of a galaxy cluster at present, containing innovative recipes for the seeding, accretion, and dynamics of supermassive black holes (SMBHs; Tremmel et al. 2017, 2019). This cluster has a virial mass of $10^{14} M_\odot$ and contains well-resolved satellite galaxies down to stellar masses of $10^8 M_\odot$. As we show, the high resolution of this simulation naturally produces ram pressure stripped tails as galaxies fall through the cluster. We find that the end of a galaxy’s star formation history is often punctuated by a brief increase in the SMBH accretion rate, which in turn heats the surrounding gas. AGN triggered by the increased ram pressure produce observable outflows, which may be important for heating the densest gas in a galaxy deep down the potential well, and in turn facilitating the quenching process. While both RPS and tidal stripping are expected to operate and cause dynamical transformations in galaxy clusters, tidal stripping effects are subdominant in the mass range of in-falling galaxies investigated here as noted in Appendix B.

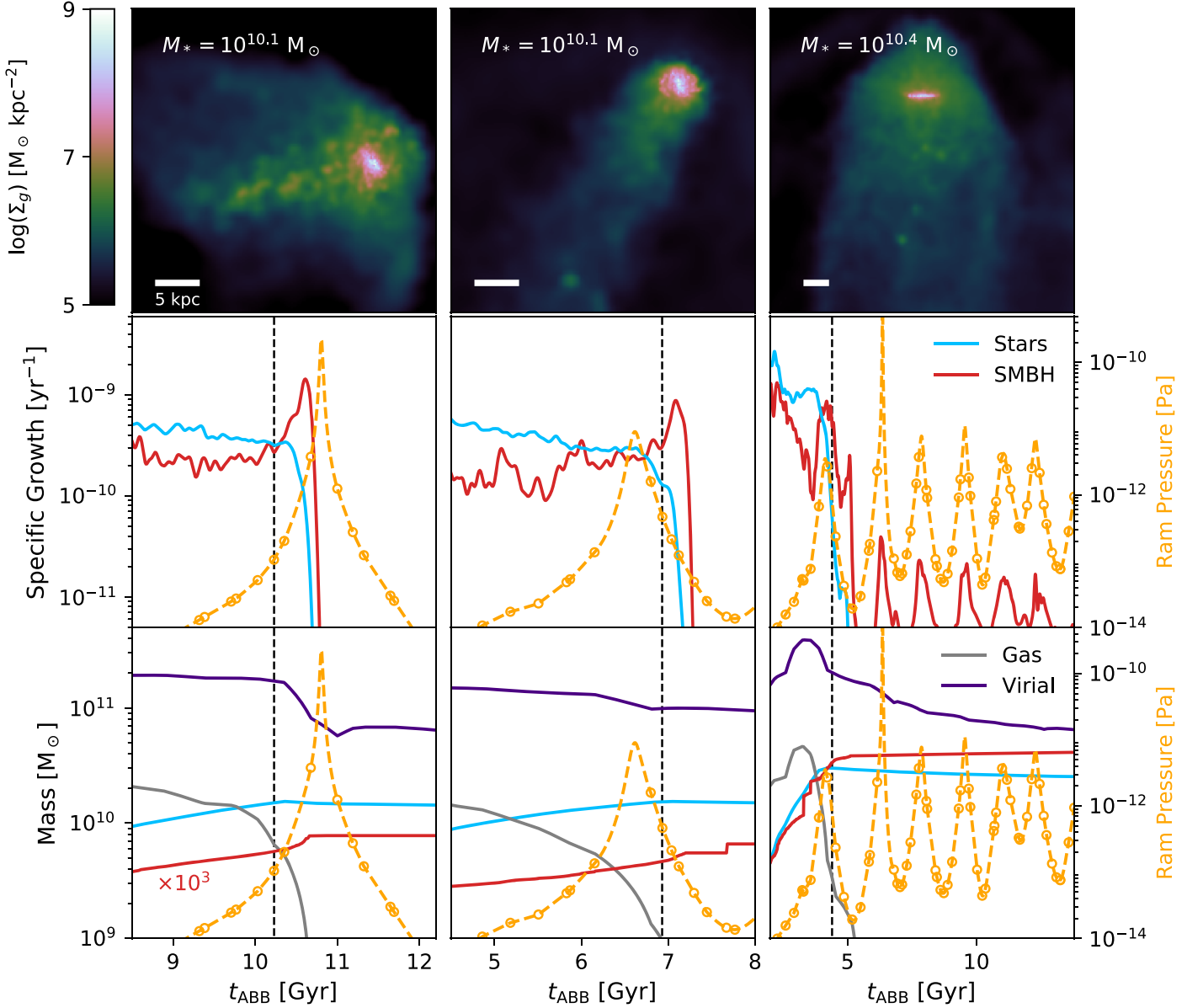


Figure 1. Three examples of enhanced AGN activity correlated with peaks in ram pressure during first pericenter passage in ROMULUSC. The top row shows a snapshot of the integrated surface mass density of the gas at the times indicated by the dashed vertical line in subsequent rows, revealing dramatic ram pressure stripped tails. The middle row plots the specific BHAR and specific SFR for these galaxies over time. The BHAR peaks just prior to quenching, marking the end of RPS. The bottom row plots the total stellar, SMBH ($\times 10^3$), virial, and bound gas mass. Ram pressure is overplotted as orange dashed curves labeled on the right-hand side. Density profiles, positions, and velocities are saved at the times marked by open circles, which are interpolated onto the finer time resolution of the BHAR and SFR.

2. Results

We find unambiguous morphological evidence of ram pressure stripping along with AGN triggering among the members of ROMULUSC. Three illustrative examples are shown in Figure 1. The top row displays gas column density maps during times marked with a dashed line in subsequent rows. The middle row displays the specific black hole accretion rate (BHAR) and star formation rate (SFR), while the bottom row displays total stellar mass, SMBH mass ($\times 10^3$), gas mass, and virial mass. For readability, specific BHAR and SFR are smoothed with a Gaussian kernel with a standard deviation of 30 Myr. The orange dashed curves show the incident ram pressure inferred from Equation (B1) (Gunn et al. 1972). Since both ambient density and galaxy velocities increase with

decreasing clustercentric radius, a peak in ram pressure corresponds to a pericenter passage. Open circles mark snapshot times at which densities and velocities are output; these curves are inferred by interpolating gas density profiles and position–velocity data over time.

In these three examples, the gas mass of in-falling cluster members is unbound within one orbit, impacted much more strongly by the cluster environment than either stellar or virial mass. This confirms that RPS dominates over tidal stripping, which would remove dark matter and stars to a greater degree than gas. The BHAR peaks during the final phases of RPS, while star formation in the galaxy quenches.⁷ Peaks in the

⁷ Note that a common definition of a quenched galaxy is a specific SFR below 10^{-11} yr^{-1} .

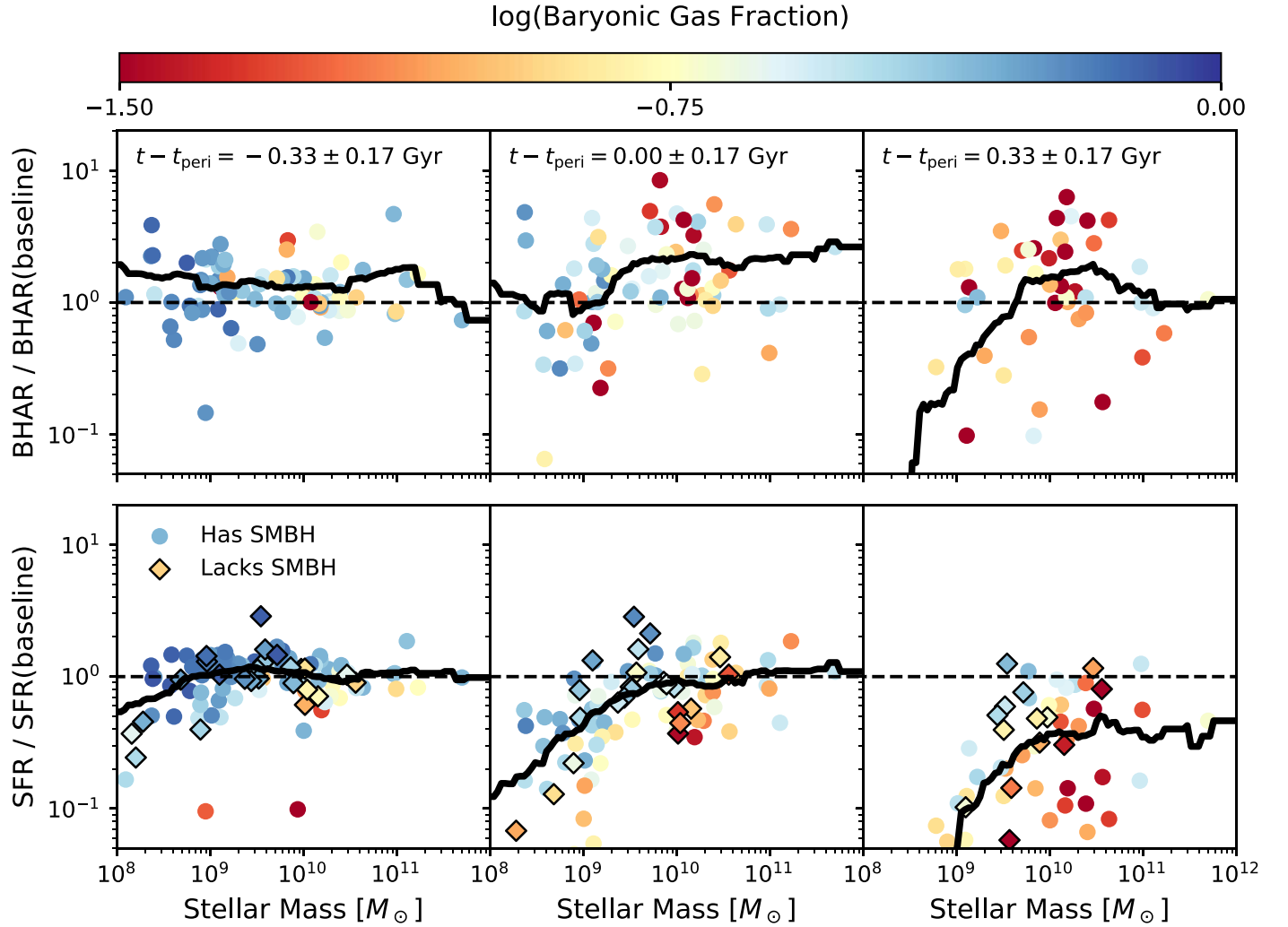


Figure 2. Evolution of BHAR and SFR during pericenter passage compared to baseline values 0.5–1.0 Gyr prior to pericenter passage. The black line shows a running average with a window 1 dex in size in M_* . During pericenter passage, for galaxies with stellar masses $>10^{9.5} M_\odot$, the BHAR is enhanced on average by a factor of 2.2. The SFR is suppressed more strongly in less massive galaxies.

specific BHAR occur near, but not exactly aligned with, peaks in ram pressure. As we show in Section 3, AGN-driven winds help evacuate the final remnants of gas during the last phases of the stripping process. In the third example, the most massive of the three, the galaxy is able to retain a very small amount of gas after the first orbit. Each time the galaxy passes pericenter, it resumes low-level AGN activity (peak Eddington ratios of $\approx 10^{-2}$ to 10^{-3}). Similar behavior has been noted in a simulation of the formation of a compact elliptical galaxy (without a SMBH), resulting in central starbursts (Du et al. 2019). While this is the most dramatic example of repetitive SMBH fueling at pericenter passage, we notice similar behavior in three other cluster members, all of relatively high stellar mass.

2.1. BHAR and SFR during Pericenter Passage

In Figure 2, we examine the evolution of the BHAR and SFR around pericenter passage for the population of cluster members as a whole. For each galaxy with a central SMBH, we first identify first pericenter passage by calculating the first time a galaxy experiences a ram pressure maximum with a peak value of at least 10^{-13} Pa. Since galaxies sometimes have

messy orbital interactions with other cluster members, this definition helps avoid uncertainties in defining pericenter based on minima in clustrocentric radius, for example. We then average the BHAR and SFR for time periods before, during, and after pericenter passage, and take the ratio with respect to baseline values. Baseline values are defined as the averages over 0.5 to 1.0 Gyr prior to pericenter passage, counting only times during which the galaxy has bound gas. We remove one outlier: a massive galaxy that is quenched prior to reaching its pericenter, but resumes forming stars at a modest rate during pericenter passage, resulting in an SFR enhancement of 7×10^4 .

Figure 2 displays the evolution of BHAR and SFR throughout first pericenter passage, averaged over time periods noted on the top of each panel. Points are color-coded according to the galaxy’s baryonic gas fraction, defined as $M_g/(M_g + M_*)$ where M_g and M_* are the bound gas and stellar mass respectively. The black curve represents a running average with a window size of 1 dex in stellar mass. On average, the BHAR is enhanced by a factor of 1.6 during pericenter passage. However, counting only galaxies above stellar masses of $10^{9.5} M_\odot$, the average enhancement rises to a factor of 2.2. Below this mass, both the BHAR and SFR are

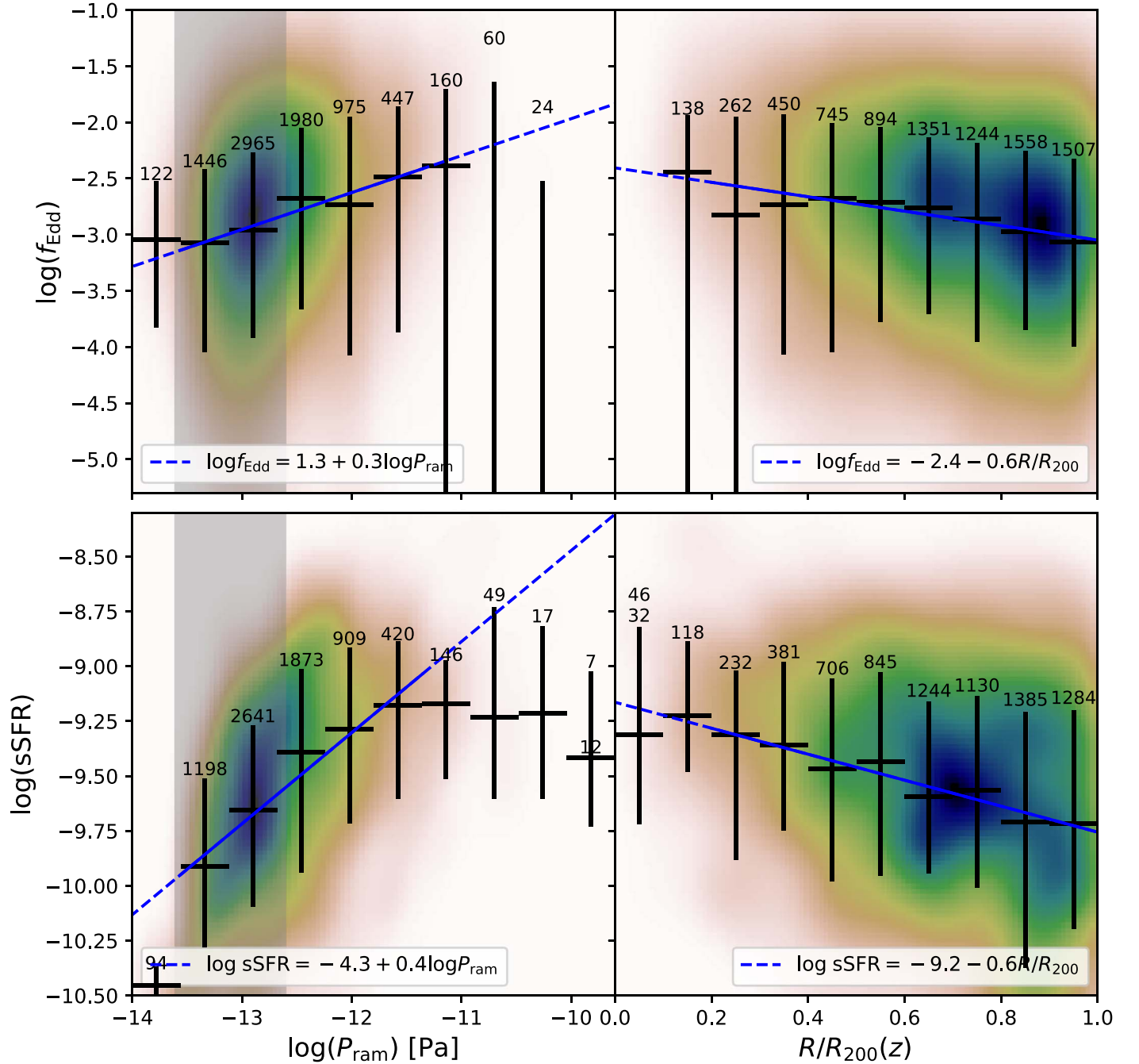


Figure 3. Eddington ratios (top) and specific star formation rates (bottom) vs. ram pressure (left) and cluster-centric distance (right) for progenitors of $z = 0$ cluster members. We include only the initial phases of RPS, while the galaxy has at least 50% of the gas with which it entered the cluster, intentionally excluding the later quenched stages. Numbers above each bin indicate the number of data points in the bin. The gray band is the region posited to trigger AGN by Marshall et al. (2018). Clear correlations are found, consistent with ram pressure systematically elevating both sSFR and f_{Edd} .

already suppressed before pericenter. Lower mass galaxies are more rapidly transformed by the RPS process than more massive galaxies with stronger gravitational potentials. Interestingly, the two galaxies that exhibit the largest enhancements of the SFR during pericenter (seen clearly in the lower panel plots) both lack a central SMBH. At later times, BHARs remain elevated in massive galaxies while the SFR is universally suppressed across a wide range of stellar masses. This is consistent with the outside-in picture of RPS, which removes star-forming gas in the outskirts of galaxies earlier than it removes the central gas that fuels SMBHs.

2.2. BHAR and SFR during Early Ram Pressure Stripping

Idealized wind-tunnel simulations predict that the SFR may increase by factors of a few during the early phases of RPS as the gas is compressed (Kronberger et al. 2008; Kapferer et al. 2009; Tonnesen & Bryan 2009; Bekki 2014). In addition, Marshall et al. (2018) used a semianalytic model to reproduce the spatial distributions of AGN in clusters and found the best agreement if AGN were triggered when $2.5 \times 10^{-14} \text{ Pa} < P_{\text{ram}} < 2.5 \times 10^{-13} \text{ Pa}$ and $P_{\text{ram}}/P_{\text{int}} > 2$, where P_{int} is the galaxy’s internal pressure support. To test these results with ROMULUSC, we attempt to find correlations

between Eddington ratio, specific SFR, ram pressure, and cluster-centric radius by searching through all of the values spanned by the cluster members in ROMULUSC. First, we trace back the main progenitor branches of every cluster member with stellar masses above $10^8 M_\odot$ at $z = 0$. For this particular analysis, the BHAR is averaged over short 10 Myr intervals, and we treat each of these intervals as an independent point. In this way, we assume that these galaxies sample the physically allowed parameter space over time. We only include time intervals during which the galaxy is within the cluster and retains at least 50% of the gas mass with which it entered. We impose this criterion to isolate the initial enhancement of BHAR with ram pressure, and to exclude the later stages when the lack of gas naturally leads to low f_{Edd} and sSFR.

In Figure 3, we plot Eddington ratio and specific star formation rate versus the host galaxy’s incident ram pressure and cluster-centric distance. The heat map represents the distribution of 10 Myr data points spanned by the galaxies in ROMULUSC over time. These distributions are then binned as a function of ram pressure, and the 16th, 50th, and 84th percentiles are marked with black error bars. The numbers above these error bars indicate the number of points in the bin. In these early phases, both f_{Edd} and sSFR clearly increase with increasing ram pressure. These trends appear to plateau at the most extreme ram pressures. However, we caution that these bins have comparatively far fewer data points, many of which come from the same individual galaxy histories, and interpolating galaxy positions may lead one to infer erroneously high ram pressures during pericenter. Similar trends are seen in the right column with cluster-centric distance. Higher values of f_{Edd} and sSFR are more likely at small cluster-centric distances, where the ram pressure is higher. The gray bar shows the range of ram pressure proposed to trigger AGN by Marshall et al. (2018). Rather than a threshold, our results appear more consistent with a smooth increase in f_{Edd} with incident ram pressure, extending to larger values of ram pressure. In blue, we plot the result of a linear regression to the bins containing at least 200 points. We note that these distributions contain long, non-Gaussian tails toward low values of Eddington ratio. Bearing this in mind, we fit only the binned $\pm 1\sigma$ values and treat the scatter as Gaussian rather than fitting the data points directly to avoid biasing results toward the most extreme outliers, those being galaxies with extremely low f_{Edd} or sSFR. We obtain the following fits for ram pressure triggered AGN activity and star formation rate while a galaxy retains at least 50% of its gas mass at infall:

$$\begin{aligned}\log_{10} f_{\text{Edd}} &= 1.3 + 0.3 \log_{10} P_{\text{ram}} \pm 0.9 \\ \log_{10} \text{sSFR} &= -4.3 + 0.4 \log_{10} P_{\text{ram}} \pm 0.4 \\ \log_{10} f_{\text{Edd}} &= -2.4 - 0.6(R/R_{200}) \pm 1.0 \\ \log_{10} \text{sSFR} &= -9.2 - 0.6(R/R_{200}) \pm 0.5,\end{aligned}$$

where the values following the \pm sign are the average $1 - \sigma$ scatter in dex among bins with at least 200 points, weighted by the number of points in the bin. While more massive galaxies are preferentially more likely to retain their gas reservoirs through periods of higher ram pressure, to ensure that the above obtained correlations are not driven by this, we check and report that stellar mass is not the main driver of these relations. We reproduce this plot for narrow intervals of stellar mass and confirm that these correlations persist, although the numerical values of the weights shift slightly.

3. A Case Study: RPS with and without an SMBH

Like most modern hydrodynamical simulations of galaxy formation, ROMULUSC includes AGN feedback, which is believed to be necessary to prevent gas from over-cooling in massive halos (e.g., Croton et al. 2006; Kormendy & Ho 2013). It naturally acts on the gas deepest in the galaxy’s potential well, which is the most difficult gas for RPS to remove. By heating and driving winds that radially redistribute this gas to the outer parts of the galaxy, AGN feedback can make this gas more susceptible to stripping.

ROMULUSC produces a pair of similar galaxies that we study in more detail to better understand the relationship between ram pressure, quenching, and AGN. These two galaxies each have stellar masses of $10^{10.5} M_\odot$ and experience similar ram pressure over time, but one has a central SMBH and the other does not. The galaxy lacking a central SMBH only has wandering SMBHs, the most central of which is 17 kpc away at $z = 0$. While rare, this situation arises in ROMULUSC because seeding is based on local rather than halo properties, and SMBHs are not forced to stay at the centers of their halos (Tremmel et al. 2018). We compare the two galaxies in this case study in Figure 4. We plot specific SFR as thick solid lines, and the specific BHAR of the galaxy with an SMBH with a thin line. Thin dotted lines depict the ram pressure, which is remarkably similar for these two galaxies. At the times shown by the thin dashed lines, we plot temperature and velocity maps in the panels above. As these galaxies pass through pericenter, both galaxies exhibit a mild enhancement of the specific SFR. The galaxy lacking a central SMBH slowly quenches over the course of 3 Gyr. In contrast, the galaxy containing an SMBH experiences a burst of AGN activity shortly after pericenter passage. In the top row, we plot temperature and velocity maps taken after pericenter within 1 kpc wide slabs that are oriented perpendicular to the disk. These maps reveal that the AGN drives a hot outflow with speeds of hundreds of km s^{-1} , while no outflow develops in the galaxy without a central SMBH. In this case, AGN feedback heats the gas, drives a wind, disturbs the disk morphology, and may help quench the galaxy on a much shorter timescale. This strongly resembles the jellyfish galaxy JO201, which has the same stellar mass, contains a central hole of molecular gas, and exhibits an outflow of 261 km s^{-1} (George et al. 2019; Radovich et al. 2019).

4. Conclusions

We have analyzed the connection between ram pressure and AGN activity in the state-of-the-art ROMULUSC cosmological simulation of a $10^{14} M_\odot$ cluster, one of the highest resolution clusters ever simulated. We find that during peaks of ram pressure, the BHAR tends to increase by a factor of ~ 2 , even while the SFR is in decline. As long as a galaxy has gas, both the Eddington ratio and specific star formation rate in galaxies increase along with the incident ram pressure. In one case study, RPS and AGN appear to work in synergy to quench star formation. Ram pressure compresses the gas and helps fuel the AGN, which imparts energy to its surroundings to help facilitate the stripping process. This suggests that AGN feedback may play a role in rapidly quenching galaxies during the final phases of RPS.

Controlled, idealized wind-tunnel experiments of RPS containing AGN would be useful in better understanding these processes. In cosmological simulations like ROMULUSC, it is

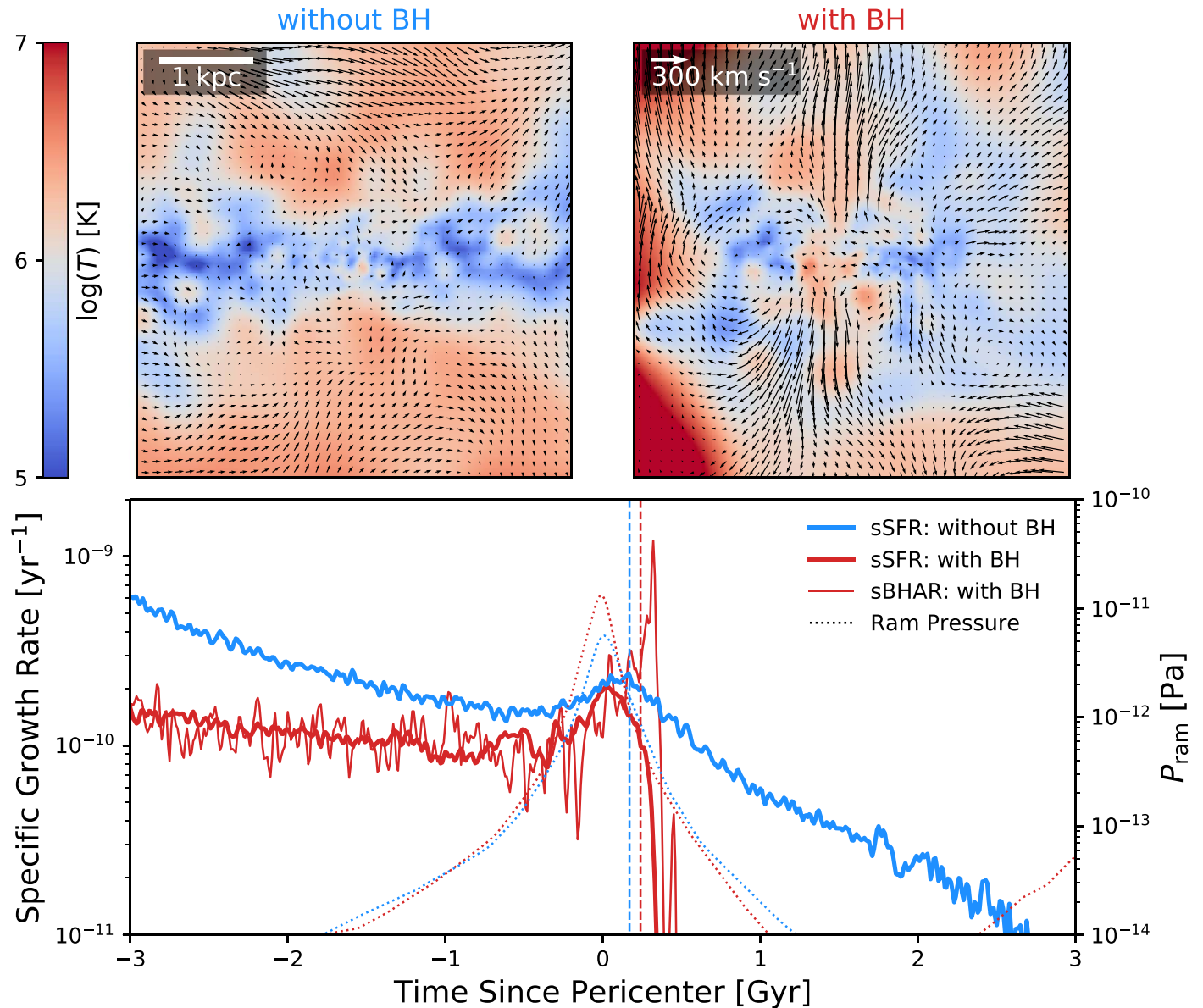


Figure 4. Case study of two similar galaxies with similar orbits, one with a central SMBH and one without. The galaxy with an SMBH experiences an enhancement of AGN activity during pericenter and rapidly quenches. The galaxy without an SMBH experiences a factor of ≈ 2 enhancement in the SFR only, and quenches much more slowly over the course of 3 Gyr. We compute temperature and velocity maps for each of these galaxies near pericenter passage, at the times marked by the dashed vertical lines. These maps reveal that AGN feedback in the galaxy with a central SMBH produces a hot outflow that helps rapidly quench the galaxy.

difficult to disentangle simultaneous processes, and many “subgrid” approximations are required to make the problem computationally feasible. Some important approximations and confounding factors are listed below:

1. The ISM: ROMULUSC lacks the resolution to fully resolve the patchy nature of the ISM. High-resolution RPS simulations indicate that stripping proceeds more efficiently with a multi-phase ISM, since wind can move through the holes in the disk (Quilis et al. 2000; Tonnesen & Bryan 2009).
2. Galactic magnetic fields: RPS simulations including a magnetic field have been shown to create more flared disks. Oblique shocks that develop between the disk and the ICM promote gas inflows to the centers of galaxies, which may help fuel AGN more efficiently (Ramos-Martínez et al. 2018). Since ROMULUSC lacks magnetic

fields, we may underestimate the AGN accretion events triggered in this way.

3. SMBH fueling and feedback: at present, neither SMBH fueling or feedback are fully understood, and there exist a variety of plausible models implemented in galaxy-scale simulations. It would be useful to determine how robust our results are to variations of these models. In particular, mechanical “radio-mode” feedback, which is not implemented in ROMULUSC, is thought to be much more efficient at removing gas, especially at low-Eddington ratios (e.g., Choi et al. 2015). This could potentially increase the effects of AGN feedback that we see at the end of the RPS process.
4. Preprocessing: most galaxies that fall into ROMULUSC are satellites in smaller substructures. For example, it is known that ROMULUSC experiences a group merger at $z \approx 0.2$ that disrupts the cluster’s cool core

(Chadayammuri et al. 2020). The total ram pressure experienced by a galaxy may therefore be underestimated since we do not take other substructures into account.

While a comprehensive comparison is beyond the scope of this work, this study helps explain the trend of elevated incidence of AGN among jellyfish galaxies (Poggianti et al. 2017) and reproduces the observed signatures attributed to AGN feedback (George et al. 2019; Radovich et al. 2019). Note that ROMULUSC is a $10^{14} M_{\odot}$ cluster, while observed clusters with jellyfish galaxies can be up to an order of magnitude more massive. We predict that in clusters of higher mass or redshift, the effects described in this work would likely occur at larger radius, due to higher ambient gas densities. We speculate that this may be relevant for the observed high incidence of AGN in the outskirts of high-redshift, massive clusters (Koulouridis & Bartalucci 2019). This work motivates more detailed and controlled studies to better understand the RPS-AGN connection using alternative techniques and subgrid models for AGN and galaxy physics.

We thank Daisuke Nagai and Mila Chadayammuri for illuminating discussions about ROMULUSC and other galaxy clusters. A.R. acknowledges support by NASA Headquarters under the NASA Earth and Space Science Fellowship Program—Grant 80NSSC17K0459, and the National Science Foundation under grant No. OISE 1743747. A.R. also thanks the black hole Initiative for its computational resources and collaborative atmosphere. P.N. acknowledges support from the National Science Foundation under TCAN 1332858. M.T. gratefully acknowledges the support of the Yale Center for Astronomy and Astrophysics Postdoctoral Fellowship.

This research is part of the Blue Waters sustained petascale computing project, which is supported by the National Science Foundation (awards OCI-0725070 and ACI1238993) and the state of Illinois. Blue Waters is a joint effort of the University of Illinois at Urbana-Champaign and its National Center for Supercomputing Applications. This work is also part of a Petascale Computing Resource Allocations allocation support by the National Science Foundation (award number OAC-1613674). This work also used the Extreme Science and Engineering Discovery Environment (XSEDE), which is supported by National Science Foundation grant No. ACI-1548562. Resources supporting this work were also provided by the NASA High-End Computing (HEC) Program through the NASA Advanced Supercomputing (NAS) Division at Ames Research Center. Analysis was conducted on the NASA Pleiades computer and facilities supported by the Yale Center for Research Computing.

Appendix A Numerical Methods

We analyze the ROMULUSC simulation, a state-of-the-art zoom-in simulation of a $10^{14} M_{\odot}$ galaxy cluster that includes AGN feedback (Tremmel et al. 2015, 2017). In previous work, we established that SMBHs and their galaxies coevolve in the ROMULUS simulations, irrespective of stellar mass, redshift, or intergalactic environment (Ricarte et al. 2019). Sharma et al. (2019) investigate the scatter about these trends for dwarf galaxies, finding that SMBH growth is affected by halo assembly history and that feedback from AGN can affect the evolution of galaxies even at low masses. Tremmel et al. (2019)

find that the cluster environment results in significantly higher quenching rates on all mass scales. Here, we briefly summarize the important and relevant gas and SMBH physics, while more details can be found in Tremmel et al. (2017, 2019).

The ROMULUSC simulations are performed using the Tree + Smoothed Particle Hydrodynamics code CHANGA (Menon et al. 2015). Gravity is softened below 350 pc using a spline kernel (equivalent to 250 pc Plummer softening), hydrodynamics are resolved to 70 pc, and gas particles have masses of $2.12 \times 10^5 M_{\odot}$. While this is sufficient resolution to produce resolved stripped tails characteristic of “jellyfish” galaxies, it is not high enough to fully resolve the patchy structure of the ISM. Magnetic fields are not included in these simulations.

SMBHs are seeded based on local gas properties, rather than simply imposing a halo mass threshold as is often adopted (e.g., Springel et al. 2005; Vogelsberger et al. 2013; Schaye et al. 2015). A gas particle designated to form a star instead forms an SMBH if it has low metallicity, high density, and a temperature of $\approx 10^4$ K, motivated by models of direct collapse black hole seeding (Haiman & Loeb 2001; Oh & Haiman 2002; Begelman et al. 2006; Lodato & Natarajan 2006). SMBHs grow from surrounding gas particles based on Bondi-Hoyle-Lyttleton (Bondi 1952) accretion, modified to account for angular momentum support. There is only one mode of AGN feedback: 2% of the radiative energy released during the accretion process (assuming a radiative efficiency of 10%) is dumped thermally into surrounding gas particles. Finally, unlike many other cosmological simulations, SMBHs are not forced by hand to stay in gravitational potential minima. Their dynamics are self-consistently followed by correcting for unresolved dynamical friction due to gravitational softening (Tremmel et al. 2015).

Appendix B Post-processing

The Amiga Halo Finder (Knollmann & Knebe 2009) is used to identify substructure—halos, subhalos, and the galaxies at their centers. At $z = 0$, in ROMULUSC 227 cluster members exist with stellar masses of at least $10^8 M_{\odot}$ in halos with at least 10^4 dark matter particles. We trace back the histories of every cluster member of ROMULUSC using the tools available in the TANGOS database structure (Pontzen & Tremmel 2018), which uses particle tracking to identify halo merger trees. The BHAR and SFR are each saved with a resolution of 10 Myr, while most other properties are only saved at each larger snapshot, of which there are 72 spaced between $z = 12.88$ and $z = 0$. Importantly, these less frequently output quantities include each galaxy’s coordinates and gas particle data. These are interpolated onto the same time resolution as the BHAR and SFR. To estimate the magnitude of ram pressure, we use the formula of Gunn et al. (1972):




$$P_{\text{ram}} \approx \rho_{\text{ICM}}(R)v^2, \quad (\text{B1})$$

where $\rho_{\text{ICM}}(R)$ is the ambient gas mass density of the ICM, R is the distance of the in-falling galaxy with respect to the cluster center, and v the velocity of the in-falling galaxy relative to cluster center. To avoid ambiguities in the computation of these quantities locally, we compute ρ_{ICM} based on spherically averaged density profiles of the cluster gas (which excludes gas in satellite galaxies), and compute v relative to that of the center of the dark matter halo of the cluster, which is computed using

a shrinking spheres method. For a more realistic situation of a turbulent ICM, this analytic calculation may tend to underestimate the true relative velocity between galaxies and surrounding gas.

We note that tidal stripping is expected to become more important than RPS only in galaxies that are at least $\approx 1/8$ the mass of the cluster (McCarthy et al. 2008). For ROMULUSC with a cluster mass of $10^{14} M_{\odot}$ and galaxies with the total masses in the range $10^{9-12.5} M_{\odot}$ (with stellar masses in the range of $10^{8-11} M_{\odot}$) considered here, we expect RPS effects to dominate over tidal stripping.

ORCID iDs

Angelo Ricarte  <https://orcid.org/0000-0001-5287-0452>
 Michael Tremmel  <https://orcid.org/0000-0002-4353-0306>
 Priyamvada Natarajan  <https://orcid.org/0000-0002-5554-8896>

References

- Barnes, J. E. 2002, *MNRAS*, **333**, 481
 Begelman, M. C., Volonteri, M., & Rees, M. J. 2006, *MNRAS*, **370**, 289
 Bekki, K. 2014, *MNRAS*, **438**, 444
 Blumenthal, K. A., & Barnes, J. E. 2018, *MNRAS*, **479**, 3952
 Bondi, H. 1952, *MNRAS*, **112**, 195
 Boselli, A., Cuillandre, J. C., Fossati, M., et al. 2016, *A&A*, **587**, A68
 Capelo, P. R., & Dotti, M. 2017, *MNRAS*, **465**, 2643
 Chadayammuri, U., Tremmel, M., Nagai, D., Babul, A., & Quinn, T. 2020, arXiv:2001.06532
 Choi, E., Ostriker, J. P., Naab, T., Oser, L., & Moster, B. P. 2015, *MNRAS*, **449**, 4105
 Cramer, W. J., Kenney, J. D. P., Sun, M., et al. 2019, *ApJ*, **870**, 63
 Croton, D. J., Springel, V., White, S. D. M., et al. 2006, *MNRAS*, **365**, 11
 Crowl, H. H., & Kenney, J. D. P. 2006, *ApJL*, **649**, L75
 Du, M., Debattista, V. P., Ho, L. C., et al. 2019, *ApJ*, **875**, 58
 Ebeling, H., Stephenson, L. N., & Edge, A. C. 2014, *ApJL*, **781**, L40
 George, K., Poggianti, B. M., Bellhouse, C., et al. 2019, *MNRAS*, **487**, 3102
 Gunn, J. E., Gott, J., & Richard, I. 1972, *ApJ*, **176**, 1
 Haiman, Z., & Loeb, A. 2001, *ApJ*, **552**, 459
 Kapferer, W., Sluka, C., Schindler, S., Ferrari, C., & Ziegler, B. 2009, *A&A*, **499**, 87
 Kenney, J. D. P., van Gorkom, J. H., & Vollmer, B. 2004, *AJ*, **127**, 3361
 Knollmann, S. R., & Knebe, A. 2009, *ApJS*, **182**, 608
 Kormendy, J., & Ho, L. C. 2013, *ARA&A*, **51**, 511
 Koulouridis, E., & Bartalucci, I. 2019, *A&A*, **623**, L10
 Kronberger, T., Kapferer, W., Ferrari, C., Unterguggenberger, S., & Schindler, S. 2008, *A&A*, **481**, 337
 Lodato, G., & Natarajan, P. 2006, *MNRAS*, **371**, 1813
 Marshall, M. A., Shabala, S. S., Krause, M. G. H., et al. 2018, *MNRAS*, **474**, 3615
 McCarthy, I. G., Frenk, C. S., Font, A. S., et al. 2008, *MNRAS*, **383**, 593
 Menon, H., Wesolowski, L., Zheng, G., et al. 2015, *ComAC*, **2**, 1
 Merluzzi, P., Busarello, G., Dopita, M. A., et al. 2013, *MNRAS*, **429**, 1747
 Oh, S. P., & Haiman, Z. 2002, *ApJ*, **569**, 558
 Poggianti, B. M., Fasano, G., Omizzolo, A., et al. 2016, *AJ*, **151**, 78
 Poggianti, B. M., Jaffé, Y. L., Moretti, A., et al. 2017, *Natur*, **548**, 304
 Pontzen, A., & Tremmel, M. 2018, *ApJS*, **237**, 23
 Quilis, V., Moore, B., & Bower, R. 2000, *Sci*, **288**, 1617
 Radovich, M., Poggianti, B., Jaffé, Y. L., et al. 2019, *MNRAS*, **486**, 486
 Ramos-Martínez, M., Gómez, G. C., & Pérez-Villegas, Á. 2018, *MNRAS*, **476**, 3781
 Ricarte, A., Tremmel, M., Natarajan, P., & Quinn, T. 2019, *MNRAS*, **489**, 802
 Schaye, J., Crain, R. A., Bower, R. G., et al. 2015, *MNRAS*, **446**, 521
 Schulz, S., & Struck, C. 2001, *MNRAS*, **328**, 185
 Sharma, R., Brooks, A., Somerville, R. S., et al. 2019, arXiv:1912.06646
 Springel, V., di Matteo, T., & Hernquist, L. 2005, *MNRAS*, **361**, 776
 Tonnesen, S., & Bryan, G. L. 2009, *ApJ*, **694**, 789
 Tonnesen, S., Bryan, G. L., & van Gorkom, J. H. 2007, *ApJ*, **671**, 1434
 Tremmel, M., Governato, F., Volonteri, M., Pontzen, A., & Quinn, T. R. 2018, *ApJL*, **857**, L22
 Tremmel, M., Governato, F., Volonteri, M., & Quinn, T. R. 2015, *MNRAS*, **451**, 1868
 Tremmel, M., Karcher, M., Governato, F., et al. 2017, *MNRAS*, **470**, 1121
 Tremmel, M., Quinn, T. R., Ricarte, A., et al. 2019, *MNRAS*, **483**, 3336
 van Gorkom, J. H. 2004, in *Clusters of Galaxies: Probes of Cosmological Structure and Galaxy Evolution*, ed. J. S. Mulchaey, A. Dressler, & A. Oemler (Cambridge: Cambridge Univ. Press), **305**
 Vogelsberger, M., Genel, S., Sijacki, D., et al. 2013, *MNRAS*, **436**, 3031
 Vollmer, B., Cayatte, V., Balkowski, C., & Duschl, W. J. 2001, *ApJ*, **561**, 708
 Vulcani, B., Poggianti, B. M., Gullieuszik, M., et al. 2018, *ApJL*, **866**, L25